Published in final edited form as:
Am J Physiol Heart Circ Physiol. 2020 October 01; 319(4): H775–H786. doi:10.1152/ajpheart.00415.2020.

p38δ genetic ablation protects female mice from anthracycline cardiotoxicity

Sharon A. George[1], **Alexi Kiss**[2,3], **Sofian N. Obaid**[1], **Aileen Venegas**[1], **Trisha Talapatra**[1], **Chapman Wei**[2,4], **Tatiana Efimova**[2,3,4], **Igor R. Efimov**[1,3]

[1]Department of Biomedical Engineering, The George Washington University, Washington, District of Columbia;

[2]Department of Anatomy and Cell Biology, The George Washington University School of Medicine and Health Sciences, Washington, District of Columbia;

[3]The George Washington Cancer Center, Washington, District of Columbia;

[4]Department of Dermatology, The George Washington University School of Medicine and Health Sciences, Washington, District of Columbia

Abstract

The efficacy of an anthracycline antibiotic doxorubicin (DOX) as a chemotherapeutic agent is limited by dose-dependent cardiotoxicity. DOX is associated with activation of intracellular stress signaling pathways including p38 MAPKs. While previous studies have implicated p38 MAPK signaling in DOX-induced cardiac injury, the roles of the individual p38 isoforms, specifically, of the alternative isoforms p38γ and p38δ, remain uncharacterized. We aimed to determine the potential cardioprotective effects of p38γ and p38δ genetic deletion in mice subjected to acute DOX treatment. Male and female wild-type (WT), p38$\gamma^{-/-}$, p38$\delta^{-/-}$, and p38$\gamma^{-/-}\delta^{-/-}$ mice were injected with 30 mg/kg DOX and their survival was tracked for 10 days. During this period, cardiac function was assessed by echocardiography and electrocardiography and fibrosis by Picro Sirius Red staining. Immunoblotting was performed to assess the expression of signaling proteins and markers linked to autophagy. Significantly improved survival was observed in p38$\delta^{-/-}$ female mice post-DOX relative to WT females, but not in p38$\gamma^{-/-}$ or p38$\gamma^{-/-}\delta^{-/-}$ male or female mice. The improved survival in DOX-treated p38$\delta^{-/-}$ females was associated with decreased fibrosis, increased cardiac output and LV diameter relative to DOX-treated WT females, and similar to saline-treated controls. Structural and echocardiographic parameters were either unchanged or worsened in all other groups. Increased autophagy, as suggested by increased LC3-II level, and decreased mammalian target of rapamycin activation was also observed in DOX-treated p38$\delta^{-/-}$ females. p38δ plays a crucial role in promoting DOX-induced cardiotoxicity in female mice by

Correspondence: T. Efimova (tefimova@gwu.edu).

AUTHOR CONTRIBUTIONS

S.A.G., A.K., T.E., and I.R.E. conceived and designed research; S.A.G., A.K., S.N.O., A.V., T.T., and C.W. performed experiments; S.A.G., A.K., S.N.O., T.T., C.W., T.E., and I.R.E. analyzed data; S.A.G., A.K., T.E., and I.R.E. interpreted results of experiments; S.A.G. and T.E. prepared figures; S.A.G. and T.E. drafted manuscript; S.A.G., A.K., T.E., and I.R.E. edited and revised manuscript; S.A.G., A.K., S.N.O., A.V., T.T., C.W., T.E., and I.R.E. approved final version of manuscript.

DISCLOSURES

No conflicts of interest, financial or otherwise, are declared by the authors.

inhibiting autophagy. Therefore, p38δ targeting could be a potential cardioprotective strategy in anthracycline chemotherapy.

NEW & NOTEWORTHY This study for the first time identifies the sex-specific roles of the alternative p38γ and p38δ MAPK isoforms in promoting doxorubicin (DOX) cardiotoxicity. We show that p38δ and p38γ/δ systemic deletion was cardioprotective in female but not in male mice. Cardiac structure and function were preserved in DOX-treated p38δ$^{-/-}$ females and autophagy marker was increased.

Keywords

cardioprotection; doxorubicin; p38 MAPK; p38δ/MAPK13; sex differences

INTRODUCTION

The anthracycline antibiotic doxorubicin (DOX) is a highly potent chemotherapeutic agent that is widely used for the treatment of many different types of cancers such as sarcoma, lymphoma, leukemia, and breast cancer. However, the efficient use of DOX is limited by the development of dose-dependent, life-threatening cardiomyopathy, leading to congestive heart failure, which can occur within a year (early onset) or several years or even decades (late-onset) after DOX treatment (7, 34, 51). This poses a unique problem because not only are heart disease and cancer listed as the two leading causes of mortality in the United States (16), but treatment of one condition contributes to the prevalence of the other.

The pathophysiological mechanisms of DOX-induced cardiotoxicity remain incompletely understood. Accumulating evidence implicates genotoxic stress associated with DOX-mediated induction of double-strand DNA breaks through inhibition of topoisomerase 2β (63, 65), oxidative stress due to increased generation of reactive oxygen species (ROS) and antioxidant depletion (17, 18), inflammation (15, 60), as well as mitochondrial and autophagy dysregulation (12, 22, 28) in DOX-induced cardiac injury, leading to cardiomyocyte dysfunction and cell death.

DOX-induced systemic inflammation and ROS generation activate stress signaling pathways in multiple cell types, including cardiomyocytes, immune cells, endothelial cells, and stromal fibroblasts, by upregulating and activating Toll-like receptors (TLRs). TLRs are involved in cardiac stress response and inflammatory signaling, and substantially contribute to the pathology of DOX-induced cardiac injury (30, 40, 44). In cardiac myocytes, activation of TLR signaling leads to downstream activation of the p38 mitogen-activated protein kinase (MAPK) family that controls adaptive responses to stresses in mammalian cells (30). p38 MAPK isoforms p38α, p38β, p38γ, and p38δ have tissue-specific expression patterns and context-dependent functions (8). The redundant, distinct, and even opposing functions of each p38 isoform have been reported (32, 64). p38α and p38β, referred to as the conventional p38 isoforms, have been studied more extensively, while the specialized functions of p38γ and p38δ, known as the alternative p38 isoforms, are less understood, in part, due to the lack of inhibitors specific to these isoforms (9).

All four p38 MAPK isoforms are expressed in the heart (8, 32, 64). p38α and p38β appear to play opposite roles in cardiac apoptosis and cardiac hypertrophy regulation (61), while p38γ and p38δ have been reported to control cardiac growth by promoting mammalian target of rapamycin (mTOR) activation through phosphorylation and degradation of the mTOR inhibitor protein DEPTOR (13).

Although p38 MAPK signaling has been implicated in DOX-induced cardiotoxicity, the roles of the individual p38 isoforms in regulating the mechanisms underlying the cardiotoxic side effects of DOX remain thus far uncharacterized. Thus, previous approaches, such as a simultaneous co-inhibition of either a subset [for example, using a pharmacological inhibitor specific for p38α/p38β (4)], or all four p38 isoforms [for instance, using a dominant-negative mutant approach (54)] confounded the analysis of the reported phenotypes. Moreover, the roles of p38γ and p38δ in anthracycline cardiotoxicity have not been explored previously.

In this study, we investigated the roles of the alternative p38 isoforms p38γ and p38δ in DOX-induced cardiotoxicity using systemic p38γ, p38δ or p38γ/p38δ knockout mice.

METHODS

All animal protocols were approved by the Institutional Animal Care and Use Committee at The George Washington University and conform to the guidelines of the National Institutes of Health's *Guide for the Care and Usage of Laboratory Animals*. Raw data files will be made available upon request.

Mouse strains.

All mice used in this study were on a C57BL/6J background. Wild-type (WT) mice were ordered from the Jackson Laboratory (stock no. 000664). Generation of mice with systemic deletion of p38γ and p38δ or both genes was previously reported, and these mice are viable and fertile and display no discernable abnormalities (46). Genotyping was carried out as described (46). Mice with systemic deletion of p38γ and p38δ were bred in-house to generate mice that lacked p38γ ($p38\gamma^{-/-}$), p38δ ($p38\delta^{-/-}$), and both p38γ and p38δ ($p38\gamma^{-/-}\delta^{-/-}$). The efficient knockdown of p38γ and p38δ was confirmed by Western blot analysis (Supplemental Fig. S3B; https://doi.org/10.6084/m9.figshare.12640613; note: all supplemental material in this article may be found at the same repository). Male and female mice were used in experiments at ~15 wk of age at the time of DOX administration. An overview of the mouse genotypes used in this study and the treatments they were subjected to are illustrated in Fig. 1A. Cardiac function was previously characterized in these mutant mice at 9 wk of age and was found to be normal (13).

Survival protocol.

The study protocol is illustrated in Fig. 1B. Mice were injected intraperitoneally (ip) with either 20 or 30 mg/kg of DOX, or saline (vehicle control), and the survival of the mice and their health status were tracked over the next 10 days. While 20 mg/kg of DOX treatment is a frequently used dose to study DOX-induced cardiotoxicity in mouse models (54, 61), we did not observe any significant changes in survival or cardiac function after administration of

this dose over 10–15 days of observation in any of our experimental groups. Hence, we used a higher dose in this study, 30 mg/kg of DOX, which effectively replicated the previously described cardiotoxic response. Following the administration of DOX, each day over a period of 10 days, mice were assigned a number between 1 and 0 to indicate their health status based on a previously published mouse health metric (6). A health score of 1 indicated a healthy mouse with no visible signs of distress, 0.75 indicated slight impairment such as slight hunch in posture, 0.5 indicated a sick mouse that was hunched and showed slow movement, 0.25 indicated a moribund mouse, and 0 indicated a dead mouse. During the 10-day survival period, cardiac function was assessed on *days 5* and *10* by echocardiography and electrocardiography as indicated in Fig. 1B. On *day 10*, the surviving mice were euthanized and their hearts were collected following thoracotomy and either fixed in 4% paraformaldehyde for histological assessment or flash frozen in liquid nitrogen for protein extraction for Western blot analysis.

Electrocardiography.

On *days 5* and *10* post-DOX injection, electrocardiography (ECG) was recorded from the surviving mice in the conscious state using the noninvasive emka ECG tunnel recording device (emka Technologies, Paris, France). Briefly, mice were guided into a mouse size-specific tunnel over a platform fitted with four ECG electrodes. The mouse was positioned on the platform such that the four paws were in contact with the electrodes, and the ECG was recorded using IOX software. The recorded signals were then analyzed using a custom Matlab program to determine P wave duration (P), P-R interval (PR), QRS duration (QRS), QT interval corrected for heart rate (HR; QTc), and R-R interval (RR).

Echocardiography.

After ECG measurements, mice were anesthetized by inhalation of 2.5% isoflurane at 1 ml/min oxygen flow using an EZ anesthesia machine. Once unresponsive, the mice were transferred to an imaging stage fitted with ECG electrodes to measure HR. Isoflurane level was adjusted between 1 and 2.5% to maintain a HR of ~400 beats/min, except in sick mice where HR was reduced irrespective of anesthesia. Chest hair was removed, and ultrasound gel (Aquasonics, Clear) was applied on the chest, left of the sternum. M-mode echocardiography of the left ventricle (LV) was performed using the Vevo 3100 system (VisualSonics, Fujifilm), and the acquired data were analyzed using VevoLAB2.1.0. Ejection fraction (EF), cardiac output (CO), stroke volume (SV), fractional shortening (FS), LV posterior wall thickness during systole (LVPWs) and diastole (LVPWd), and LV end systolic and diastolic diameters (LVESD and LVEDD, respectively) were measured.

Histology.

At the end of the survival period, mice were euthanized and hearts were collected and fixed in 4% paraformaldehyde for 48 h and then transferred to 70% ethanol. Hearts were then paraffin embedded, sectioned onto slides in the cross-sectional orientation and stained using the Picro Sirius Red as per the manufacturer’s instructions (Abcam), to assess collagen deposition. Slides were then imaged using a light microscope and three images each from the LV and right ventricle (RV), from the base, mid and apex regions, were acquired. The images were analyzed using a custom MatLab program to determine the percentage of area

occupied by collagen (red) in both the LV and RV. The average collagen content (visualized by Picro Sirius Red staining) as a percentage of total imaged area was determined for the base, mid and apex regions, and was quantified and averaged for the LV and RV separately. Thus, each data point reported here is an average of three images per heart.

Western blot analysis.

Hearts isolated from mice were rinsed in PBS to remove blood and flash frozen in liquid nitrogen. Ventricular tissue was cut from these frozen sections and lysed in RIPA lysis buffer (89901, Sigma) supplemented with protease and phosphatase inhibitor tablets (A32955, ThermoFisher). Total protein concentration was determined using a BCA kit (23227, Thermo Scientific) following the manufacturer's instructions. Electrophoresis was performed to separate the proteins on a 4–15% Bio-Rad Criterion gel (5671084, Bio-Rad) and transferred to a polyvinylidene difluoride membrane. Membranes were then blocked using Odyssey Blocking buffer (927–5000, Li-Cor) and incubated overnight in primary antibodies at 4°C. Membranes were then washed and incubated with secondary antibodies for 2 h at room temperature. Membranes were washed again and imaged using a Li-Cor FC imager, and protein expression was measured using Image Studio Lite software. All protein expressions are normalized to GAPDH to account for loading errors. In the case of LC3 bands, the density of each band was quantified separately and normalized to GAPDH. Primary antibodies used in this study include p38α (M0800, 1:1,000, Sigma-Aldrich), p38γ (2307, 1:500, Cell Signaling), p38δ (MRC PPU, 1:300, University of Dundee), mTOR (2972, 1:1,000, Cell Signaling), phospho-mTOR Ser2488 (5535, 1:500, Cell Signaling), Akt (4691, 1:1,000, Cell Signaling), phospho-Akt Th308 (13038, 1:500, Cell Signaling), DEPTOR (NBP1–49674, 1:1,000, Novus Biologicals), LC3 (TA301542, 1:500, Origene), GAPDH (ab9484, 1:1,000, Abcam) and α-tubulin (4074, 1:1,000, Abcam). Secondary antibodies used in this study include IRDye 680 Donkey antimouse (926–68022, Li-Cor) and IRDye 800 Donkey anti-rabbit (926–32213, Li-Cor).

Statistics.

All data are reported as means ± SD unless stated otherwise. Sample sizes are listed in the figures. Log rank tests were performed to determine statistically significant differences in the mouse survival data. For all other data sets, significance was determined by one-way ANOVA with genotype as the single factor, and Student's *t* tests were performed for post hoc analysis. A P value < 0.05 was considered statistically significant.

RESULTS

Female p38δ $^{-/-}$ mice are protected against DOX-induced mortality and morbidity.

Activation of p38 MAPK in hearts of WT male mice acutely treated with DOX has been previously demonstrated (21, 53). We first examined whether the p38 MAPK signaling pathway was activated in WT female mice treated with DOX at 30 mg/kg. As shown in Supplemental Fig. S1A, we detected a significant increase in phosphorylation/activation of p38 MAPK as well as of the upstream activators (MKK3 and MKK6) and downstream effectors (p53 and HSP27) of the p38 MAPKs in DOX-treated versus saline-treated WT mouse hearts. These data indicate a sustained (lasting for at least 5 days) activation of the

p38 MAPK signaling pathway by DOX treatment in our mouse model. Of note, all four p38 isoforms could potentially contribute to this activation. We also observed a significant increase in p38δ protein expression in female, but not in male, WT mice treated with DOX versus saline, whereas no significant change in p38γ protein expression was observed in DOX-treated male or female mice. These results suggest that p38δ might be involved in DOX-induced cardiotoxicity in female mice.

We next investigated the in vivo roles of p38γ and p38δ in the DOX-induced acute cardiotoxicity model using genetic loss-of-function approach. WT, p38$\gamma^{-/-}$, p38$\delta^{-/-}$, and p38$\gamma^{-/-}\delta^{-/-}$ male and female mice were treated with DOX at 20 or 30 mg/kg of body weight (DOX20 and DOX30, respectively) by ip injection, as outlined in Fig. 1, A and B. The survival and health of mice were tracked over the next 10 days. While all mice treated with saline (control, black line, Fig. 1C) survived the acute survival period, those treated with DOX had varying responses depending on their genotype and sex, as well as the dose of DOX.

The survival rates were not significantly affected by treatment with DOX20 relative to control in any of the experimental groups (Fig. 1C, *left*). In contrast, the acute survival was significantly reduced in all groups treated with DOX30 relative to control, except in female p38$\delta^{-/-}$ mice (Fig. 1C, *right*). Among WT mice treated with DOX30, only 40% of males and no females survived the 10-day period post-DOX. In the p38$\gamma^{-/-}$ mice, a 20% survival rate and in the p38$\gamma^{-/-}\delta^{-/-}$ mice, a 10% survival rate were observed in both males and females. Remarkably, while only 20% of DOX30-treated male p38$\delta^{-/-}$ mice survived the acute survival period, 80% of female p38$\delta^{-/-}$ mice survived. These findings suggest that p38δ is a crucial determinant of DOX cardiotoxicity in female mice.

Notably, significant sex-dependent differences in survival were observed as early as 5 days post-DOX injection. As shown in Supplemental Table 1, the 5-day survival rates of DOX30-treated male WT, p38$\delta^{-/-}$, and p38$\gamma^{-/-}\delta^{-/-}$ mice were significantly lower compared with their respective female counterparts.

To determine whether DOX-induced morbidity correlated with mortality, we additionally tracked the health status of the DOX-treated mice over the 10-day survival period, as detailed in METHODS (Fig. 1D). Comparing the survival data and the health status (Fig. 1, C vs. D), demonstrates that although the survival rates were not significantly reduced in mice treated with DOX20, the surviving mice were of poor health, especially male and female p38$\gamma^{-/-}$ mice (Fig. 1D, *left*). Among mice treated with DOX30, survival rates correlated with health status across genotypes. Importantly, the higher survival rate seen in the female p38$\delta^{-/-}$ group correlated with better health status similar to controls (Fig. 1D, *bottom right*).

DOX-treated female p38δ $^{-/-}$ mice exhibit preserved cardiac function.

Cardiac function deteriorates due to DOX-induced cardiotoxicity. We next assessed cardiac mechanical function in DOX30-treated WT, p38$\gamma^{-/-}$, p38$\delta^{-/-}$, and p38$\gamma^{-/-}\delta^{-/-}$ male and female mice by M-mode echocardiography. Data obtained 5 days post-DOX treatment are shown in Fig. 2 and Table 1.

Ejection fraction (EF) and fractional shortening (FS) were not significantly altered in the DOX30-treated male or female mice of any of the genotypes examined. This lack of EF and FS response to DOX treatment was also observed in few surviving female mice at *day 10* post-DOX30 treatment (Supplemental Fig. S2).

Importantly, a major indicator of DOX cardiotoxicity in our mouse model was a significant reduction in cardiac output (CO). CO was significantly reduced in all DOX30-treated female mice, while a significant CO decrease in males was only observed in the p38$\delta^{-/-}$ and p38$\gamma^{-/-}\delta^{-/-}$ groups. A rapid progression of cardiotoxicity, high mortality rates, and large variations in CO response to DOX in the DOX30-treated male WT and p38$\gamma^{-/-}$ groups may have contributed to the lack of significant CO response in these groups. To further test this, we assessed cardiac mechanical function at an earlier time point (*day 3*) in male DOX30-treated WT mice. As expected, CO was significantly reduced in DOX30-treated WT males on *day 3* post-treatment (Supplemental Fig. S3). Of note, even though CO was significantly reduced in all DOX30-treated groups of female mice relative to saline-treated controls, DOX30-treated p38$\delta^{-/-}$ females (which displayed a higher survival rate) had a significantly higher CO compared with DOX30-treated WT female mice, suggesting an amelioration of DOX cardiotoxicity in this group.

Next, LV parameters such as wall thickness and diameter were measured to assess heart failure due to DOX treatment. Among DOX30-treated male mice, LV parameters were altered only in p38$\gamma^{-/-}\delta^{-/-}$ mice, where LV wall thickness (LVPWD) was increased and LV diameter (LVEDD) was correspondingly decreased (Fig. 2C). On the other hand, among DOX30-treated female mice, LV wall thickness was increased only in the p38$\gamma^{-/-}$ group while LV diameters in systole and diastole (LVESD and LVEDD, respectively) were significantly reduced in DOX30-treated WT, p38$\gamma^{-/-}$, and p38$\gamma^{-/-}\delta^{-/-}$ groups. In keeping with their higher survival rates and better health status, DOX30-treated female p38$\delta^{-/-}$ mice exhibited preserved LV parameters, both wall thickness and diameter, similar to saline-treated controls.

To summarize the echocardiographic analysis, cardiac mechanical function and LV wall structure were significantly perturbed by DOX treatment in male and female mice of all genotypes included in this study, except in female p38$\delta^{-/-}$ mice (Fig. 2), in line with the improved health and survival rate observed in this group.

ECG parameters are preserved in DOX-treated female p38δ $^{-/-}$ mice.

The effects of DOX treatment on cardiac electrophysiology were determined by recording ECGs in conscious mice. Illustrated and summarized in Fig. 3 and Table 1 are ECG traces and parameters from mice treated with DOX30 5 days post-DOX.

Once again, a significant modulation of cardiac function by DOX was mostly measurable only in female, but not in male mice. (Fig. 3C and Table 1). Electrophysiological response to DOX-treatment in female mice was rather complex. For example, the P wave interval, an indicator of speed of electrical excitation spread over the atria, was shortened in DOX30-treated WT female mice, but prolonged in DOX30-treated p38$\gamma^{-/-}\delta^{-/-}$ females. This opposite response in WT and p38$\gamma^{-/-}\delta^{-/-}$ groups could be due to a combination of the

effects of DOX treatment and the combined p38γ and p38δ genetic deletion and requires further investigation. On the other hand, QRS duration, an indicator of speed of electrical excitation spread over the ventricles, was prolonged in DOX30-treated p38$\gamma^{-/-}$ female mice alone, although a trend toward QRS prolongation was also observed in DOX30-treated WT females. Importantly, ECG parameters in DOX30-treated female p38$\delta^{-/-}$ female mice were similar to saline-treated controls.

Lastly, HR from DOX30-treated mice was measured in both conscious and anesthetized states. Once again, significant HR changes due to DOX treatment were largely observed in female mice. In conscious mice, HR was significantly reduced in DOX-treated p38$\gamma^{-/-}\delta^{-/-}$ female mice relative to control. On the other hand, in anesthetized mice, HR was significantly reduced in all DOX30-treated female mice relative to control (Fig. 3C and Table 1). Differential HR response to DOX treatment in the conscious versus anesthetized state requires further investigation. Next, HR from the same mouse was compared between the conscious versus anesthetized states. It is well established that isoflurane anesthesia reduces HR (62). Notably, a significant HR reduction in the anesthetized versus conscious state was detected only in WT male and female mice, both saline and DOX30-treated, as well as in DOX30-treated p38$\delta^{-/-}$ female mice. The lack of significant changes in HR between the conscious and anesthetized states in the p38$\gamma^{-/-}$ and p38$\gamma^{-/-}\delta^{-/-}$ groups could be due to a trend toward a lower HR in the conscious state seen in these groups to begin with.

Fibrosis is reduced in hearts of DOX-treated female p38δ $^{-/-}$ and p38$\gamma^{-/-}\delta^{-/-}$ mice.

Extracellular edema and fibrosis are commonly observed during several cardiac diseases, including heart failure (38, 39, 48). DOX treatment has previously been shown to induce fibrosis in the heart (25, 28). We next assessed myocardial collagen deposition in mice treated with DOX30 on *day 10* posttreatment using Picro Sirius Red staining (Fig. 4). Fibrosis in left and right ventricles (LVs and RVs) was evaluated separately in female mice of all groups (Fig. 4B). Male mice were not included due to high mortality rate in this group at *day 10* post-DOX.

As expected, increased fibrosis, demonstrated by enhanced Picro Sirius Red staining, was observed in the LV of female WT mice treated with DOX relative to controls. Notably, LV fibrosis in DOX30-treated female p38$\delta^{-/-}$ and p38$\gamma^{-/-}\delta^{-/-}$ mice was significantly reduced relative to DOX30-treated female WT mice and was similar to control values. Interestingly, DOX treatment did not change fibrosis in the RV of mice in any of the DOX30-treated groups relative to control (Fig. 4B, *right*). The observed preservation of cardiac structure in the DOX30-treated female p38$\delta^{-/-}$ mice was in keeping with the improved health and survival as well as the preservation of cardiac function in this group.

p38δ deletion results in reduced mTOR activation and increased autophagic marker in hearts of DOX-treated female mice.

DOX cardiotoxicity has been linked to dysregulation of autophagy in the myocardium (3, 25). mTOR signaling has been shown to regulate autophagy, specifically, to provide maladaptive feedback inhibition of DOX-induced autophagy in the heart (28). Notably, p38γ

and p38δ have been implicated in the control of mTOR activity in the heart by means of phosphorylation and subsequent degradation of the mTOR-inhibitory protein DEPTOR (13). We therefore examined the potential effect of the individual or combined p38δ and p38γ deletion on myocardial mTOR/Akt signaling and autophagy in DOX30-treated female mice 10 days post-DOX treatment.

As illustrated in Fig. 5, A and B, the expression of total mTOR protein and the phosphorylation of mTOR at Ser 2488 were significantly reduced in DOX30-treated female p38$\delta^{-/-}$ mice relative to DOX30-treated female WT mice, as assessed by immunoblotting. On the other hand, no significant changes were detected in total Akt protein expression or in Akt phosphorylation at Thr308. However, Akt phosphorylation at Ser473 was significantly reduced in all DOX30-treated female mice relative to control (Fig. 5, A and B). No changes in DEPTOR or LC3-I expression were observed in any of the groups of female mice (Fig. 5, A and B). Of note, the lack of an increase in DEPTOR protein expression in any of the knockout strains relative to WT is at variance with the previously published data (13), possibly due to different experimental settings. Finally, as shown in Fig. 5B, the levels of LC3-II, a marker of autophagosome formation, were significantly increased in female p38$\delta^{-/-}$ and p38$\gamma^{-/-}\delta^{-/-}$ mice relative to control. No significant changes in the expression or phosphorylation of the proteins specified in Fig. 5A were detected in DOX30-treated male mutant mice versus their saline-treated control counterparts (data not shown). These data suggest that the resistance of female p38$\delta^{-/-}$ mice to DOX cardiotoxicity could be at least partly ascribed to the loss of the mTOR-dependent negative regulation of DOX-stimulated autophagic response.

Interestingly, DOX30-treated female p38$\gamma^{-/-}\delta^{-/-}$ mice exhibited protected phenotypes such as reduced fibrosis and increased autophagy marker expression even though this group had lower survival rates relative to controls 10 days post-DOX30 treatment. However, in a separate survival experiment using groups of older female mice (22 wk of age), p38$\gamma^{-/-}\delta^{-/-}$ females fared significantly better with DOX20 treatment, exhibiting a 100% survival rate compared with 60% survival rate in the DOX20-treated WT female cohort (Supplemental Fig. S4A). A significant increase in the autophagy marker LC3-II was also observed in this group (Supplemental Fig. S4C). This suggests that the combined deletion of both p38γ and p38δ, while beneficial at lower DOX doses, cannot sustain normal cardiac function at higher DOX doses. The pathways involved in the development of cardiotoxicity in this group will require further investigation.

DISCUSSION

In this study we investigated the roles of stress-activated alternative p38 MAPK isoforms p38γ and p38δ in the development of cardiotoxic effects induced by treatment with the anthracycline antibiotic DOX. We report that a systemic genetic deletion of p38δ protects female mice against DOX-induced cardiotoxicity. Our findings, summarized in Fig. 6, revealed that cardiac electrical and mechanical functions were preserved in female mice lacking p38δ, resulting in a significantly higher survival rate 10 days after DOX30 injection compared with WT female mice (80 vs. 0%, $P < 0.05$). One mechanism that could contribute

to cardioprotection in this group could be increased autophagy as suggested by an increase in protein expression of the autophagic marker LC3-II.

Sex-dependent differences in anthracycline cardiotoxicity.

Clinical and animal studies that investigated the role of sex as a risk factor in anthracycline cardiotoxicity have yielded confounding results. Sex as a risk factor has been extensively studied among childhood cancer patients treated with anthracyclines. However, these studies have reported varying results such as studies that identified female sex as a significant risk factor (2, 26, 29, 49), others that report no sex differences in anthracycline-induced cardiotoxicity (41, 56), and yet others that report ventricular dysfunction in males subjected anthracycline therapy (57). The role of sex in anthracycline-induced cardiotoxicity in adults is less explored because the majority of the anthracycline-treated adult patients are women diagnosed with breast cancer (33). However, the preponderance of clinical studies in adult patients and preclinical animal studies report male sex as a significant risk factor in the development of cardiotoxicity after anthracycline treatment (19, 33, 35–37). Consistently, we report here that regardless of genotype, adult male mice treated with DOX displayed an average of 45% survival rate 5 days post-DOX while in female groups an average of 86% mice survived this time period. One of the important novel findings of this study is the sex-dependent roles of alternative p38 MAPK isoforms in cardiotoxicity and survival. Sex hormone differences could underlie the sexual dimorphism reported here. For example, it has been reported that, while estrogen treatment and estrous-staged therapy suppressed DOX-induced cardiotoxicity in rats, testosterone and progesterone did not have any effects (42, 43, 66). The mechanisms underlying the sex-dependent differences in responses to anthracycline therapy undoubtedly merit further investigation.

Preserved EF during DOX treatment.

While it is well established that reduced EF is a hallmark of DOX treatment, transient changes in EF especially during early phases of chemotherapy have also been reported (50, 55). No change or even improvement in EF immediately after the first cycle of chemotherapy have been reported in patients (50, 55). In our acute DOX treatment model, we observed preserved EF in all groups of mice treated with DOX at *days 3* and *5* post-DOX treatment. One possible explanation for this phenomenon could be the simultaneous modulation of both systolic and diastolic function by DOX. To elucidate this further, EF is calculated using the ratio of blood ejected from the heart during systole to the maximal LV loading during diastole. Reduced systolic ejection and diastolic loading at the same time can result in preserved EF. Of note, DOX has been reported to cause both systolic and diastolic dysfunction (5, 67).

The acute, transient changes in EF could complicate early diagnosis of DOX-induced cardiotoxicity using this metric. On the other hand, in our mouse model, CO was acutely reduced in males and females after DOX treatment, suggesting that reduced CO could serve as an earlier indicator of DOX cardiotoxicity.

Stress signaling in DOX cardiotoxicity.

Generation of ROS is suggested as one of the potential mechanisms underlying anthracycline-induced cardiotoxicity (17, 18). Increased ROS generation has multiple downstream effects that can contribute to development of heart failure symptoms such as mitochondrial dysfunction, altered intracellular calcium homeostasis, and apoptosis among others, resulting in a significant impairment of cardiac electrical and mechanical functions. Previous in vivo studies have implicated p38 MAPK signaling in DOX cardiotoxicity (4, 54, 58). Most of these studies focused mainly on the conventional p38α and p38β isoforms, employing a specific inhibitor of p38α/p38β, SB203580, as a tool to delineate the contributions of these isoforms to DOX cardiotoxicity (4, 58). On the other hand, transgenic overexpression of a dominant-negative mutant form of p38α in cardiomyocytes (54) would be expected to coinhibit all four p38 isoforms, potentially obfuscating the roles of the individual p38 isoforms given their reported diverse and at times opposing roles in controlling certain aspects of cardiac physiology and pathology (45).

In this study, we focused on the contributions of the alternative p38 isoforms, p38γ and p38δ, the roles of which have not been previously examined in the context of anthracyclineinduced cardiotoxicity. We report that, while p38γ deletion did not significantly modulate cardiac function or survival after DOX treatment, p38δ deletion resulted in significantly improved cardiac function and survival in DOX-treated female mice. Cardioprotection in female p38δ$^{-/-}$ following DOX treatment was associated with decreased mTOR protein expression and activity in the hearts of mice surviving DOX treatment, and increased expression of the autophagic marker LC3-II, suggesting the potential cardioprotective role of autophagy during DOX treatment.

Importantly, in this study we implemented systemic p38γ and p38δ deletion models. This approach provides us the advantage of identifying the effects of p38γ and/or p38δ depletion/inactivation not only in the heart but also in other cell types such as immune cells, which can in turn affect cardiac function. Furthermore, based on the results of this study, any potential therapy targeting p38δ would likely be administered systemically. Relevantly, our data demonstrate that systemic p38δ deletion does not affect normal physiology and survival of these mice, while providing significant cardioprotection in female mice during DOX treatment.

Finally, p38δ deletion has also been reported to result in anticancer effects in several mouse models of cancer development, including skin, breast, and colon cancer models (11, 23, 47, 59). Thus targeting p38δ in combination with DOX chemotherapy could have a dual benefit, potentially enhancing the anticancer effect of DOX, while providing cardioprotection, particularly in female patients.

Protective role of autophagy in DOX cardiotoxicity.

Autophagy is a housekeeping mechanism that maintains the equilibrium in the cellular environment by removing damaged or degraded components. A delicate balance in autophagy is required for efficient cellular function (14, 31). On the one hand, a decrease in autophagy can result in the accumulation of degraded products within the cell and

cause mitochondrial damage that, in turn, can lead to decreased ATP production and increased oxidative stress (10, 52). On the other hand, maladaptation in autophagy can result in autophagic cell death (1, 24). In the heart, autophagy is increased in response to aging, starvation, and in diseases such as heart failure and ischemia (3, 14, 20, 25). Autophagy activation by an mTOR inhibitor has also been reported to prevent hypertrophy (27). However, the role of autophagy in the context of anthracycline cardiotoxicity is a subject of debate (3, 25). Notably, several recent reports have demonstrated that increased autophagy is protective against DOX cardiotoxicity (25, 28). Phosphoinositide 3-kinase-γ (PI3Kγ) inhibition has been shown to ameliorate DOX cardiotoxicity by means of enhanced autophagic disposal of DOX-damaged mitochondria (28). Furthermore, DOX has been found to activate a PI3Kγ/Akt/mTOR signaling pathway to promote feedback inhibition of autophagy (28). Interestingly, hearts from mice lacking p38γ, p38δ, or both isoforms have been reported to have low activity of mTOR due to high levels of the mTOR inhibitor DEPTOR (13). Consistent with these studies, our present findings uncovered a decrease in mTOR activity, as evidenced by reduced mTOR-Ser2488 phosphorylation, as well as an increase in LC3-II, a marker of autophagosome formation, in DOX-treated hearts of female p38δ$^{-/-}$ mice that were protected from DOX-induced cardiotoxicity. These results suggest that mechanistically, cardioprotection against DOX seen in female p38δ$^{-/-}$ mice could potentially be linked to enhanced autophagy resulting from a decrease in the mTOR-dependent negative feedback inhibiting the autophagy triggered by DOX. Taken together the results of this and previous studies implicate mTOR-dependent control of DOX-stimulated autophagy pathway as a crucial regulatory axis in DOX-induced cardiotoxicity. However, further studies are needed to elucidate the molecular details of this regulation. Specifically, it would be instructive to determine whether the inhibition of PI3Kγ in conjunction with p38δ ablation would lead to enhanced cardioprotective effects in female mice.

Limitations.

This study was designed based on the well-established and widely used DOX-induced acute cardiac injury model, and involved an administration of a single dose of DOX (20 or 30 mg/kg) delivered via an ip injection to mice, followed by an acute survival monitoring period of 10 days. To better mimic human chemotherapeutic regimens, we intend to employ a chronic DOX treatment regimen in our future studies, in which mice are treated with multiple smaller doses of DOX over a prolonged survival period (28, 65).

Treatment of WT mice with 20 mg/kg ip DOX has been reported to elicit acute cardiotoxicity associated with significant mortality during a 10- to 15-day period following DOX administration (54, 60). However, we did not observe any significant changes in survival after 20 mg/kg DOX was administered to 15-wk-old mice of any genotype examined, necessitating the usage of a higher dose of DOX (30 mg/kg) in our present study. The differential susceptibility to DOX20 could be due to differences in the genetic background and/or age of the mice used in different studies. Our present work showed that, in contrast to 15-wk-old mice, 22-wk-old female WT mice are in fact susceptible to DOX20-induced cardiotoxicity. Clearly, further investigation is warranted of the impact of age on DOX-triggered cardiomyopathy. Additionally, it also needs to be noted that clinical

administration of DOX involves multiple injections over a number of weeks, as well as an intravenous route of DOX administration.

Furthermore, the systemic nature of DOX treatment and genetic manipulation does not allow for the investigation of individual cell types' contribution to cardiotoxicity. Thus, additional studies are warranted that would focus on the contributions of different cardiac cell types, such as cardiomyocytes, endothelial cells, immune cells, and fibroblasts, using conditional cell type-specific knockout mouse models. Finally, while in this study we focused on cardiac function, contributions of other organ failures to DOX-induced lethality cannot be ruled out and would require further exploration.

Conclusions.

In this study, we uncovered the crucial sex-specific role of the p38δ MAPK in anthracycline cardiotoxicity. We report that systemic genetic deletion of p38δ protected female mice against DOX-induced cardiotoxicity. p38δ deletion resulted in improved cardiac mechanical and electrical function and thereby increased rate of survival in DOX-treated female mice. The improved cardiac function correlated with reduced fibrosis and enhanced autophagy.

Supplementary Material

Refer to Web version on PubMed Central for supplementary material.

ACKNOWLEDGMENTS

We acknowledge the excellent technical assistance provided by Aaron Koppel, Loubna Al Dammad, and Christian Miccile for this study.

GRANTS

This project was supported by the Leducq Foundation Project RHYTHM (to I. R. Efimov), The George Washington University Cross Disciplinary Research Fund (to I. R. Efimov and T. Efimova), and American Heart Association Post-doctoral Fellowship Grant 19POST34370122 (to S. A. George).

REFERENCES

1. Akazawa H, Komazaki S, Shimomura H, Terasaki F, Zou Y, Takano H, Nagai T, Komuro I. Diphtheria toxin-induced autophagic cardiomyocyte death plays a pathogenic role in mouse model of heart failure. J Biol Chem 279: 41095–41103, 2004. doi:10.1074/jbc.M313084200. [PubMed: 15272002]
2. Armstrong GT, Liu Q, Yasui Y, Neglia JP, Leisenring W, Robison LL, Mertens AC. Late mortality among 5-year survivors of childhood cancer: a summary from the Childhood Cancer Survivor Study. J Clin Oncol 27: 2328–2338, 2009. doi:10.1200/JCO.2008.21.1425. [PubMed: 19332714]
3. Bartlett JJ, Trivedi PC, Pulinilkunnil T. Autophagic dysregulation in doxorubicin cardiomyopathy. J Mol Cell Cardiol 104: 1–8, 2017. doi:10.1016/j.yjmcc.2017.01.007. [PubMed: 28108310]
4. Bernstein D, Fajardo G, Zhao M, Urashima T, Powers J, Berry G, Kobilka BK. Differential cardioprotective/cardiotoxic effects mediated by β-adrenergic receptor subtypes. Am J Physiol Heart Circ Physiol 289: H2441–H2449, 2005. doi:10.1152/ajpheart.00005.2005. [PubMed: 16040722]
5. Bu'Lock FA, Mott MG, Oakhill A, Martin RP. Left ventricular diastolic function after anthracycline chemotherapy in childhood: relation with systolic function, symptoms, and pathophysiology. Br Heart J 73: 340–350, 1995. doi:10.1136/hrt.73.4.340. [PubMed: 7756067]

6. Burkholder T, Foltz C, Karlsson E, Linton CG, Smith JM. Health evaluation of experimental laboratory mice. Curr Protoc Mouse Biol 2: 145–165, 2012. doi:10.1002/9780470942390.mo110217. [PubMed: 22822473]
7. Chatterjee K, Zhang J, Honbo N, Karliner JS. Doxorubicin cardiomyopathy. Cardiology 115: 155–162, 2010. doi:10.1159/000265166.
8. Court NW, dos Remedios CG, Cordell J, Bogoyevitch MA. Cardiac expression and subcellular localization of the p38 mitogen-activated protein kinase member, stress-activated protein kinase-3 (SAPK3). J Mol Cell Cardiol 34: 413–426, 2002. doi:10.1006/jmcc.2001.1523. [PubMed: 11991731]
9. Cuenda A, Sanz-Ezquerro JJ. p38γ and p38δ: from spectators to key physiological players. Trends Biochem Sci 42: 431–442, 2017. doi:10.1016/j.tibs.2017.02.008. [PubMed: 28473179]
10. De Meyer GR, De Keulenaer GW, Martinet W. Role of autophagy in heart failure associated with aging. Heart Fail Rev 15: 423–430, 2010. doi:10.1007/s10741-010-9166-6. [PubMed: 20383579]
11. del Reino P, Alsina-Beauchamp D, Escós A, Cerezo-Guisado MI, Risco A, Aparicio N, Zur R, Fernandez-Estévez M, Collantes E, Montans J, Cuenda A. Pro-oncogenic role of alternative p38 mitogen-activated protein kinases p38γ and p38δ, linking inflammation and cancer in colitis-associated colon cancer. Cancer Res 74: 6150–6160, 2014. doi:10.1158/0008-5472.CAN-14-0870. [PubMed: 25217523]
12. Dirks-Naylor AJ. The role of autophagy in doxorubicin-induced cardiotoxicity. Life Sci 93: 913–916, 2013. doi:10.1016/j.lfs.2013.10.013. [PubMed: 24404586]
13. González-Terán B, López JA, Rodríguez E, Leiva L, Martínez-Martínez S, Bernal JA, Jiménez-Borreguero LJ, Redondo JM, Vazquez J, Sabio G. p38γ and δ promote heart hypertrophy by targeting the mTOR-inhibitory protein DEPTOR for degradation. Nat Commun 7: 10477, 2016. doi:10.1038/ncomms10477. [PubMed: 26795633]
14. Gustafsson ÅB, Gottlieb RA. Autophagy in ischemic heart disease. Circ Res 104: 150–158, 2009. doi:10.1161/CIRCRESAHA.108.187427. [PubMed: 19179668]
15. Hajra S, Patra AR, Basu A, Bhattacharya S. Prevention of doxorubicin (DOX)-induced genotoxicity and cardiotoxicity: effect of plant derived small molecule indole-3-carbinol (I3C) on oxidative stress and inflammation. Biomed Pharmacother 101: 228–243, 2018. doi:10.1016/j.biopha.2018.02.088.
16. Heron M Deaths: Leading Causes for 2015. Natl Vital Stat Rep 66: 1–76, 2017.
17. Huang CY, Chen JY, Kuo CH, Pai PY, Ho TJ, Chen TS, Tsai FJ, Padma VV, Kuo WW, Huang CY. Mitochondrial ROS-induced ERK1/2 activation and HSF2-mediated AT_1 R upregulation are required for doxorubicin-induced cardiotoxicity. J Cell Physiol 233: 463–475, 2018. doi: 10.1002/jcp.25905. [PubMed: 28295305]
18. Ichikawa Y, Ghanefar M, Bayeva M, Wu R, Khechaduri A, Naga Prasad SV, Mutharasan RK, Naik TJ, Ardehali H. Cardiotoxicity of doxorubicin is mediated through mitochondrial iron accumulation. J Clin Invest 124: 617–630, 2014. doi:10.1172/JCI72931.
19. Jenkins GR, Lee T, Moland CL, Vijay V, Herman EH, Lewis SM, Davis KJ, Muskhelishvili L, Kerr S, Fuscoe JC, Desai VG. Sex-related differential susceptibility to doxorubicin-induced cardiotoxicity in $B6C3F_1$ mice. Toxicol Appl Pharmacol 310: 159 –174, 2016. doi: 10.1016/j.taap.2016.09.012. [PubMed: 27644598]
20. Kanamori H, Takemura G, Maruyama R, Goto K, Tsujimoto A, Ogino A, Li L, Kawamura I, Takeyama T, Kawaguchi T, Nagashima K, Fujiwara T, Fujiwara H, Seishima M, Minatoguchi S. Functional significance and morphological characterization of starvation-induced autophagy in the adult heart. Am J Pathol 174: 1705–1714, 2009. doi:10.2353/ajpath.2009.080875. [PubMed: 19342365]
21. Kang YJ, Zhou ZX, Wang GW, Buridi A, Klein JB. Suppression by metallothionein of doxorubicin-induced cardiomyocyte apoptosis through inhibition of p38 mitogen-activated protein kinases. J Biol Chem 275: 13690–13698, 2000. doi:10.1074/jbc.275.18.13690. [PubMed: 10788488]
22. Kawaguchi T, Takemura G, Kanamori H, Takeyama T, Watanabe T, Morishita K, Ogino A, Tsujimoto A, Goto K, Maruyama R, Kawasaki M, Mikami A, Fujiwara T, Fujiwara H, Minatoguchi S. Prior starvation mitigates acute doxorubicin cardiotoxicity through restoration

of autophagy in affected cardiomyocytes. Cardiovasc Res 96: 456–465, 2012. doi:10.1093/cvr/cvs282. [PubMed: 22952253]

23. Kiss A, Koppel AC, Murphy E, Sall M, Barlas M, Kissling G, Efimova T. Cell type-specific p38δ targeting reveals a context-, stage-, and sex-dependent regulation of skin carcinogenesis. Int J Mol Sci 20: 1532, 2019. doi:10.3390/ijms20071532. [PubMed: 30934690]
24. Knaapen MW, Davies MJ, De Bie M, Haven AJ, Martinet W, Kockx MM. Apoptotic versus autophagic cell death in heart failure. Cardiovasc Res 51: 304–312, 2001. doi:10.1016/S0008-6363(01)00290-5. [PubMed: 11470470]
25. Koleini N, Kardami E. Autophagy and mitophagy in the context of doxorubicin-induced cardiotoxicity. Oncotarget 8: 46663–46680, 2017. doi:10.18632/oncotarget.16944. [PubMed: 28445146]
26. Krischer JP, Epstein S, Cuthbertson DD, Goorin AM, Epstein ML, Lipshultz SE. Clinical cardiotoxicity following anthracycline treatment for childhood cancer: the Pediatric Oncology Group experience. J Clin Oncol 15: 1544–1552, 1997. doi:10.1200/JCO.1997.15.4.1544. [PubMed: 9193351]
27. Kuzman JA, O'Connell TD, Gerdes AM. Rapamycin prevents thyroid hormone-induced cardiac hypertrophy. Endocrinology 148: 3477–3484, 2007. doi:10.1210/en.2007-0099. [PubMed: 17395699]
28. Li M, Sala V, De Santis MC, Cimino J, Cappello P, Pianca N, Di Bona A, Margaria JP, Martini M, Lazzarini E, Pirozzi F, Rossi L, Franco I, Bornbaum J, Heger J, Rohrbach S, Perino A, Tocchetti CG, Lima BH, Teixeira MM, Porporato PE, Schulz R, Angelini A, Sandri M, Ameri P, Sciarretta S, Lima-Júnior RC, Mongillo M, Zaglia T, Morello F, Novelli F, Hirsch E, Ghigo A. Phosphoinositide 3-kinase gamma inhibition protects from anthracycline cardiotoxicity and reduces tumor growth. Circulation 138: 696 –711, 2018. doi:10.1161/CIRCULATIONAHA.117.030352. [PubMed: 29348263]
29. Lipshultz SE, Lipsitz SR, Mone SM, Goorin AM, Sallan SE, Sanders SP, Orav EJ, Gelber RD, Colan SD. Female sex and higher drug dose as risk factors for late cardiotoxic effects of doxorubicin therapy for childhood cancer. N Engl J Med 332: 1738–1744, 1995. doi:10.1056/NEJM199506293322602. [PubMed: 7760889]

29a. Lyu YL, Kerrigan JE, Lin CP, Azarova AM, Tsai YC, Ban Y, Liu LF. Topoisomerase IIbeta mediated DNA double-strand breaks: implications in doxorubicin cardiotoxicity and prevention by dexrazoxane. Cancer Res 67: 8839–8846, 2007. doi:10.1158/0008-5472.CAN-07-1649. [PubMed: 17875725]

30. Ma Y, Zhang X, Bao H, Mi S, Cai W, Yan H, Wang Q, Wang Z, Yan J, Fan G, Lindsey ML, Hu Z. Toll-like receptor (TLR) 2 and TLR4 differentially regulate doxorubicin induced cardiomyopathy in mice. PLoS One 7: e40763, 2012. [Erratum in PLoS One 7: e40763, 2012.] doi:10.1371/journal.pone.0040763. [PubMed: 22808256]
31. Maloyan A, Robbins J. Autophagy in desmin-related cardiomyopathy: thoughts at the halfway point. Autophagy 6: 665–666, 2010. doi:10.4161/auto.6.5.12422. [PubMed: 20523125]
32. Martin ED, Bassi R, Marber MS. p38 MAPK in cardioprotection - are we there yet? Br J Pharmacol 172: 2101–2113, 2015. doi:10.1111/bph.12901. [PubMed: 25204838]
33. Meiners B, Shenoy C, Zordoky BN. Clinical and preclinical evidence of sex-related differences in anthracycline-induced cardiotoxicity. Biol Sex Differ 9: 38, 2018. doi:10.1186/s13293-018-0198-2. [PubMed: 30157941]
34. Moslehi JJ. Cardiovascular toxic effects of targeted cancer therapies. N Engl J Med 375: 1457–1467, 2016. doi:10.1056/NEJMra1100265. [PubMed: 27732808]
35. Moulin M, Piquereau J, Mateo P, Fortin D, Rucker-Martin C, Gres-sette M, Lefebvre F, Gresikova M, Solgadi A, Veksler V, Garnier A, Ventura-Clapier R. Sexual dimorphism of doxorubicin-mediated cardiotoxicity: potential role of energy metabolism remodeling. Circ Heart Fail 8: 98–108, 2015. doi:10.1161/CIRCHEARTFAILURE.114.001180. [PubMed: 25420486]
36. Myrehaug S, Pintilie M, Tsang R, Mackenzie R, Crump M, Chen Z, Sun A, Hodgson DC. Cardiac morbidity following modern treatment for Hodgkin lymphoma: supra-additive cardiotoxicity of doxorubicin and radiation therapy. Leuk Lymphoma 49: 1486–1493, 2008. doi:10.1080/10428190802140873. [PubMed: 18608873]

37. Myrehaug S, Pintilie M, Yun L, Crump M, Tsang RW, Meyer RM, Sussman J, Yu E, Hodgson DC. A population-based study of cardiac morbidity among Hodgkin lymphoma patients with preexisting heart disease. Blood 116: 2237–2240, 2010. doi:10.1182/blood-2010-01-263764. [PubMed: 20595518]
38. Navas JP, Martinez-Maldonado M. Pathophysiology of edema in congestive heart failure. Heart Dis Stroke 2: 325–329, 1993. [PubMed: 8156185]
39. Nguyen TP, Qu Z, Weiss JN. Cardiac fibrosis and arrhythmogenesis: the road to repair is paved with perils. J Mol Cell Cardiol 70: 83–91, 2014. doi:10.1016/j.yjmcc.2013.10.018. [PubMed: 24184999]
40. Nozaki N, Shishido T, Takeishi Y, Kubota I. Modulation of doxorubicin-induced cardiac dysfunction in toll-like receptor-2-knockout mice. Circulation 110: 2869–2874, 2004. doi:10.1161/01.CIR.0000146889.46519.27. [PubMed: 15505089]
41. Pein F, Sakiroglu O, Dahan M, Lebidois J, Merlet P, Shamsaldin A, Villain E, de Vathaire F, Sidi D, Hartmann O. Cardiac abnormalities 15 years and more after adriamycin therapy in 229 childhood survivors of a solid tumour at the Institut Gustave Roussy. Br J Cancer 91: 37–44, 2004. doi:10.1038/sj.bjc.6601904. [PubMed: 15162142]
42. Pokrzywinski KL, Biel TG, Rosen ET, Bonanno JL, Aryal B, Mascia F, Moshkelani D, Mog S, Rao VA. Doxorubicin-induced cardiotoxicity is suppressed by estrous-staged treatment and exogenous 17β-estradiol in female tumor-bearing spontaneously hypertensive rats. Biol Sex Differ 9: 25, 2018. doi:10.1186/s13293-018-0183-9.
43. Rattanasopa C, Kirk JA, Bupha-Intr T, Papadaki M, de Tombe PP, Wattanapermpool J. Estrogen but not testosterone preserves myofilament function from doxorubicin-induced cardiotoxicity by reducing oxidative modifications. Am J Physiol Heart Circ Physiol 316: H360–H370, 2019. doi:10.1152/ajpheart.00428.2018.
44. Riad A, Bien S, Gratz M, Escher F, Westermann D, Heimesaat MM, Bereswill S, Krieg T, Felix SB, Schultheiss HP, Kroemer HK, Tschöpe C. Toll-like receptor-4 deficiency attenuates doxorubicin-induced cardiomyopathy in mice. Eur J Heart Fail 10: 233–243, 2008. doi:10.1016/j.ejheart.2008.01.004. [PubMed: 18321777]
45. Rose BA, Force T, Wang Y. Mitogen-activated protein kinase signaling in the heart: angels versus demons in a heart-breaking tale. Physiol Rev 90: 1507–1546, 2010. doi:10.1152/physrev.00054.2009.
46. Sabio G, Arthur JS, Kuma Y, Peggie M, Carr J, Murray-Tait V, Centeno F, Goedert M, Morrice NA, Cuenda A. p38γ regulates the localisation of SAP97 in the cytoskeleton by modulating its interaction with GKAP. EMBO J 24: 1134–1145, 2005. doi:10.1038/sj.emboj.7600578. [PubMed: 15729360]
47. Schindler EM, Hindes A, Gribben EL, Burns CJ, Yin Y, Lin MH, Owen RJ, Longmore GD, Kissling GE, Arthur JSC, Efimova T. p38δ Mitogen-activated protein kinase is essential for skin tumor development in mice. Cancer Res 69: 4648–4655, 2009. doi:10.1158/0008-5472.CAN-08-4455. [PubMed: 19458068]
48. Segura AM, Frazier OH, Buja LM. Fibrosis and heart failure. Heart Fail Rev 19: 173–185, 2014. doi:10.1007/s10741-012-9365-4.
49. Silber JH, Jakacki RI, Larsen RL, Goldwein JW, Barber G. Increased risk of cardiac dysfunction after anthracyclines in girls. Med Pediatr Oncol 21: 477–479, 1993. doi:10.1002/mpo.2950210704. [PubMed: 8341214]
50. Stachowiak P, Wojtarowicz A, Milchert-Leszczyńska M, Safranow K, Falco M, Kaliszczak R, Kornacewicz-Jach Z. The paradox of the first cycle of chemotherapy-transient improvement of contractility and diastolic function after the first cycle of anthracycline-based chemotherapy: a prospective clinical trial. Oncotarget 8: 96442–96452, 2017. doi:10.18632/oncotarget.21279.
51. Swain SM, Whaley FS, Ewer MS. Congestive heart failure in patients treated with doxorubicin: a retrospective analysis of three trials. Cancer 97: 2869–2879, 2003. doi:10.1002/cncr.11407.
52. Terman A, Kurz T, Navratil M, Arriaga EA, Brunk UT. Mitochondrial turnover and aging of long-lived postmitotic cells: the mitochondrial-lysosomal axis theory of aging. Antioxid Redox Signal 12: 503–535, 2010. doi:10.1089/ars.2009.2598. [PubMed: 19650712]

53. Thandavarayan RA, Giridharan VV, Arumugam S, Suzuki K, Ko KM, Krishnamurthy P, Watanabe K, Konishi T. Schisandrin B prevents doxorubicin induced cardiac dysfunction by modulation of DNA damage, oxidative stress and inflammation through inhibition of MAPK/p53 signaling. PLoS One 10: e0119214, 2015. doi:10.1371/journal.pone.0119214. [PubMed: 25742619]
54. Thandavarayan RA, Watanabe K, Sari FR, Ma M, Lakshmanan AP, Giridharan VV, Gurusamy N, Nishida H, Konishi T, Zhang S, Muslin AJ, Kodama M, Aizawa Y. Modulation of doxorubicin-induced cardiac dysfunction in dominant-negative p38α mitogen-activated protein kinase mice. Free Radic Biol Med 49: 1422–1431, 2010. doi:10.1016/j.freeradbiomed.2010.08.005. [PubMed: 20705132]
55. Unverferth DV, Magorien RD, Unverferth BP, Talley RL, Balcerzak SP, Baba N. Human myocardial morphologic and functional changes in the first 24 hours after doxorubicin administration. Cancer Treat Rep 65: 1093–1097, 1981. [PubMed: 7296554]
56. van Dalen EC, van der Pal HJH, Kok WEM, Caron HN, Kremer LCM. Clinical heart failure in a cohort of children treated with anthracyclines: a long-term follow-up study. Eur J Cancer 42: 3191–3198, 2006. doi:10.1016/j.ejca.2006.08.005. [PubMed: 16987655]
57. Vandecruys E, Mondelaers V, De Wolf D, Benoit Y, Suys B. Late cardiotoxicity after low dose of anthracycline therapy for acute lymphoblastic leukemia in childhood. J Cancer Surviv 6: 95–101, 2012. doi:10.1007/s11764-011-0186-6. [PubMed: 21630046]
58. Venkatakrishnan CD, Tewari AK, Moldovan L, Cardounel AJ, Zweier JL, Kuppusamy P, Ilangovan G. Heat shock protects cardiac cells from doxorubicin-induced toxicity by activating p38 MAPK and phosphorylation of small heat shock protein 27. Am J Physiol Heart Circ Physiol 291: H2680–H2691, 2006. doi:10.1152/ajpheart.00395.2006. [PubMed: 16782845]
59. Wada M, Canals D, Adada M, Coant N, Salama MF, Helke KL, Arthur JS, Shroyer KR, Kitatani K, Obeid LM, Hannun YA. P38 delta MAPK promotes breast cancer progression and lung metastasis by enhancing cell proliferation and cell detachment. Oncogene 36: 6649–6657, 2017. doi:10.1038/onc.2017.274. [PubMed: 28783172]
60. Wang L, Chen Q, Qi H, Wang C, Wang C, Zhang J, Dong L. Doxorubicin-induced systemic inflammation is driven by upregulation of toll-like receptor TLR4 and endotoxin leakage. Cancer Res 76: 6631– 6642, 2016. doi:10.1158/0008-5472.CAN-15-3034. [PubMed: 27680684]
61. Wang Y, Huang S, Sah VP, Ross J Jr, Brown JH, Han J, Chien KR. Cardiac muscle cell hypertrophy and apoptosis induced by distinct members of the p38 mitogen-activated protein kinase family. J Biol Chem 273: 2161–2168, 1998. doi:10.1074/jbc.273.4.2161.
62. Yang CF, Yu-Chih Chen M, Chen TI, Cheng CF. Dose-dependent effects of isoflurane on cardiovascular function in rats. Tzu Chi Med J 26: 119–122, 2014. doi:10.1016/j.tcmj.2014.07.005.
64. Yokota T, Wang Y. p38 MAP kinases in the heart. Gene 575: 369–376, 2016. doi:10.1016/j.gene.2015.09.030. [PubMed: 26390817]
65. Zhang S, Liu X, Bawa-Khalfe T, Lu LS, Lyu YL, Liu LF, Yeh ETH. Identification of the molecular basis of doxorubicin-induced cardiotoxicity. Nat Med 18: 1639–1642, 2012. doi:10.1038/nm.2919. [PubMed: 23104132]
66. Zhang XJ, Cao XQ, Zhang CS, Zhao Z. 17β-estradiol protects against doxorubicin-induced cardiotoxicity in male Sprague-Dawley rats by regulating NADPH oxidase and apoptosis genes. Mol Med Rep 15: 2695–2702, 2017. doi:10.3892/mmr.2017.6332. [PubMed: 28447737]
67. Zuppinger C, Timolati F, Suter TM. Pathophysiology and diagnosis of cancer drug induced cardiomyopathy. Cardiovasc Toxicol 7: 61–66, 2007. doi:10.1007/s12012-007-0016-2. [PubMed: 17652805]

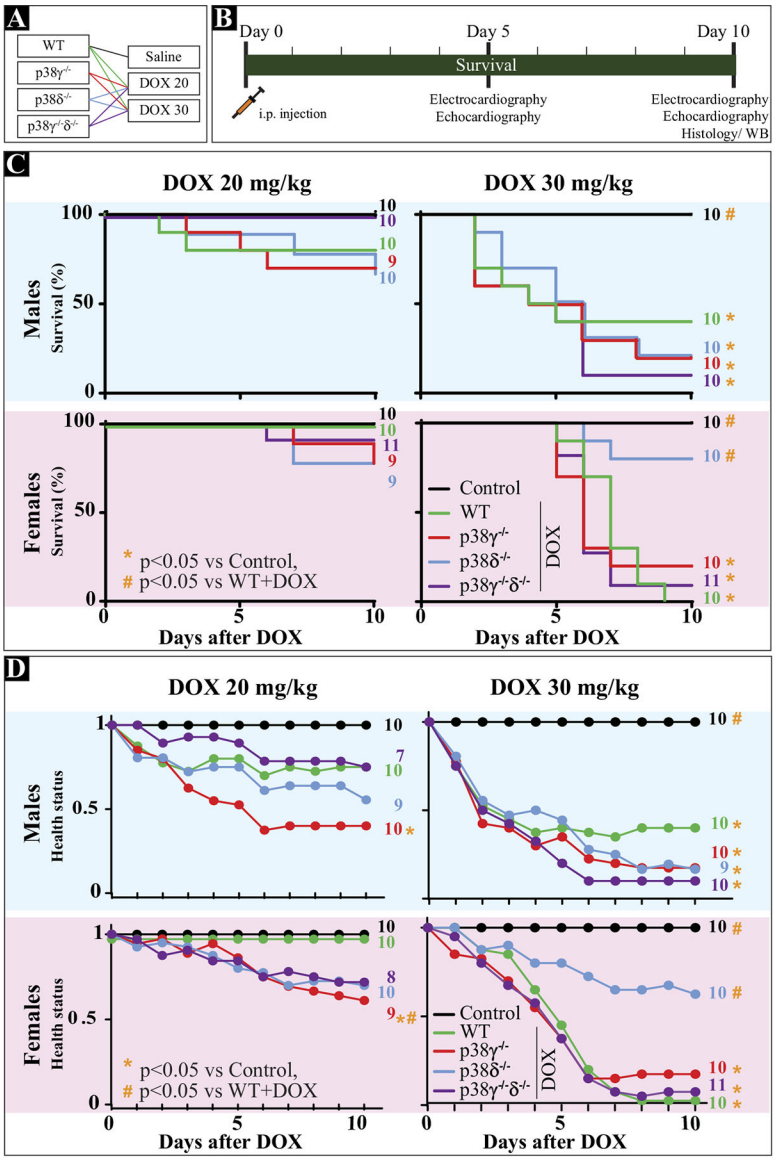

Fig. 1.

Increased survival rate and preserved health status in female p38δ$^{-/-}$ mice relative to female wild-type (WT) mice 10 days after doxorubicin (DOX) treatment. *A*: genotypes of mice used in this study and treatments they were subjected to are detailed. *B*: timeline of the experiments. Functional data from the surviving mice were acquired on *days 5* and *10* post-DOX injection, and hearts were collected for histological and protein expression assessment on *day 10*. *C*: survival rates in male and female mice (*top* and *bottom*, respectively) treated with 20 or 30 mg/kg DOX (*left* and *right*, respectively). *D*: health status was tracked in male and female mice (*top* and *bottom*, respectively) treated with 20 or 30 mg/kg DOX (*left* and *right*, respectively) over the 10-day survival period using an arbitrary health scoring system as detailed in METHODS. Log rank tests were performed to determine statistical significance. Sample size for each group is indicated beside the Kaplan–Meier curve for that group in the corresponding color (control: black, WT+DOX: green, p38γ $^{-/-}$+DOX:

red, p38$\delta^{-/-}$+DOX: blue, p38$\gamma^{-/-}\delta^{-/-}$+DOX: purple): for *C*, $n = 9–11$ mice/group; for *D*, $n = 7–11$ mice/group, as specified next to each curve. *$P < 0.05$ vs. control. #$P < 0.05$ vs. WT+DOX.

Health Research Alliance Author Manuscript

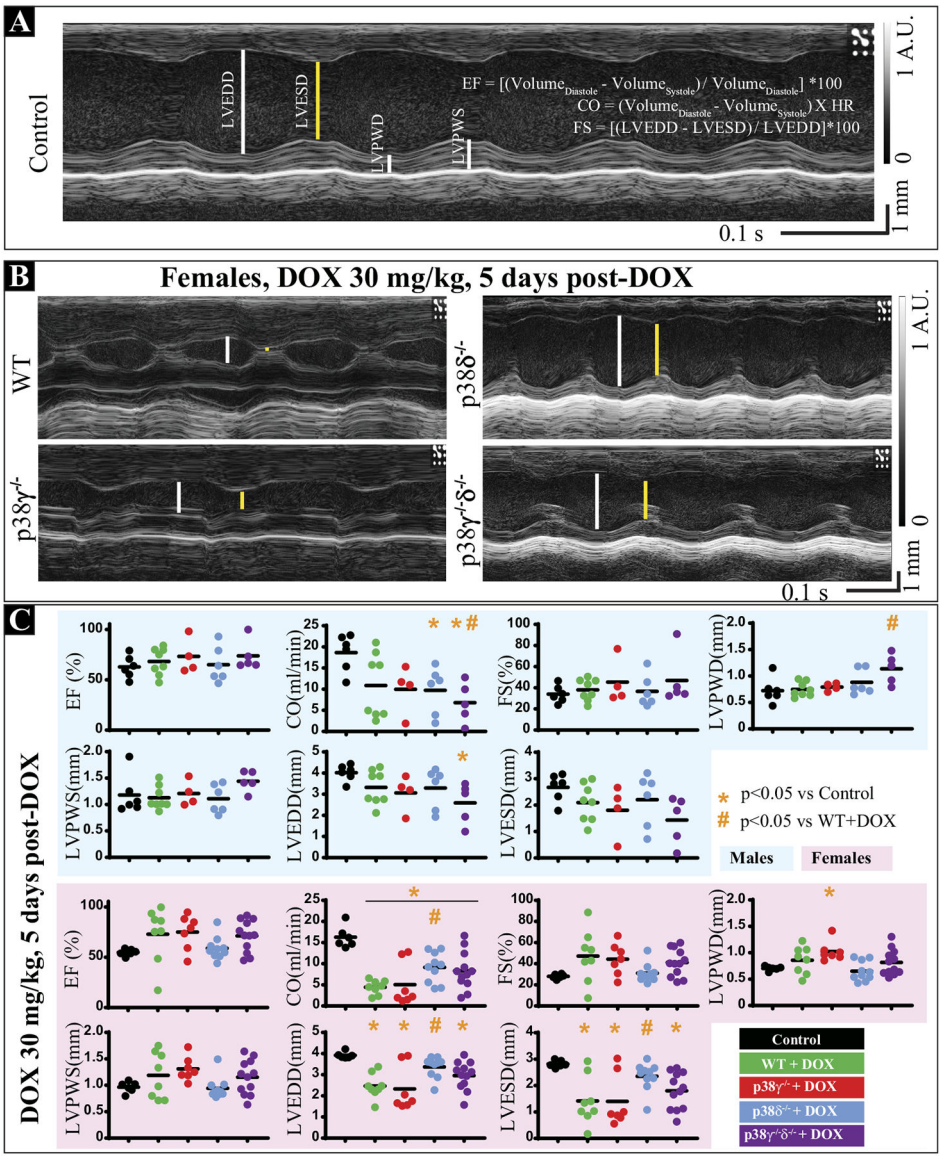

Fig. 2.

Cardiac mechanical function and left ventricular (LV) structure are preserved in doxorubicin (DOX)-treated female p38$\delta^{-/-}$ mice. *A*: representative echocardiogram from a control (saline-treated) female mouse with the description of the specific parameters measured. *B*: representative echocardiograms from female wild-type (WT), p38$\gamma^{-/-}$, p38$\delta^{-/-}$, and p38$\gamma^{-/-}\delta^{-/-}$ mice 5 days after DOX injection. *C*: indicated parameters of cardiac mechanical function were measured in male (*top*, blue) and female (*bottom*, pink) mice treated with 30 mg/kg DOX 5 days posttreatment. EF, ejection fraction, CO, cardiac output; FS, fractional shortening; LVPWD, LVPWS: left ventricular posterior wall thickness during diastole/systole; LVEDD, LVESD: left ventricular end diastolic/systolic diameter. Each color-coded circle in *C* corresponds to individual data point, one from each mouse. Average values are indicated by horizontal black line. One-way ANOVA was used to determine statistically significant differences between groups for each parameter, and 2-tailed, unpaired Student's

Health Research Alliance Author Manuscript

t tests were performed as post hoc analysis. Bonferroni correction was applied for multiple comparisons. Due to variability in survival rates 5 days post-DOX, variable, sample sizes are observed between groups. Sample sizes for each group are as follows: males, control: n = 6, WT+DOX: n = 8, p38$\gamma^{-/-}$+DOX: n = 4, p38$\delta^{-/-}$+DOX: n = 6, p38$\gamma^{-/-}\delta^{-/-}$+DOX: n = 5; females, control: n = 6, WT+DOX: n = 8, p38$\gamma^{-/-}$+DOX: n = 7, p38$\delta^{-/-}$+DOX: n = 10, p38$\gamma^{-/-}\delta^{-/-}$+DOX: n = 12. *P < 0.05 vs. control. #P < 0.05 vs. WT+DOX.

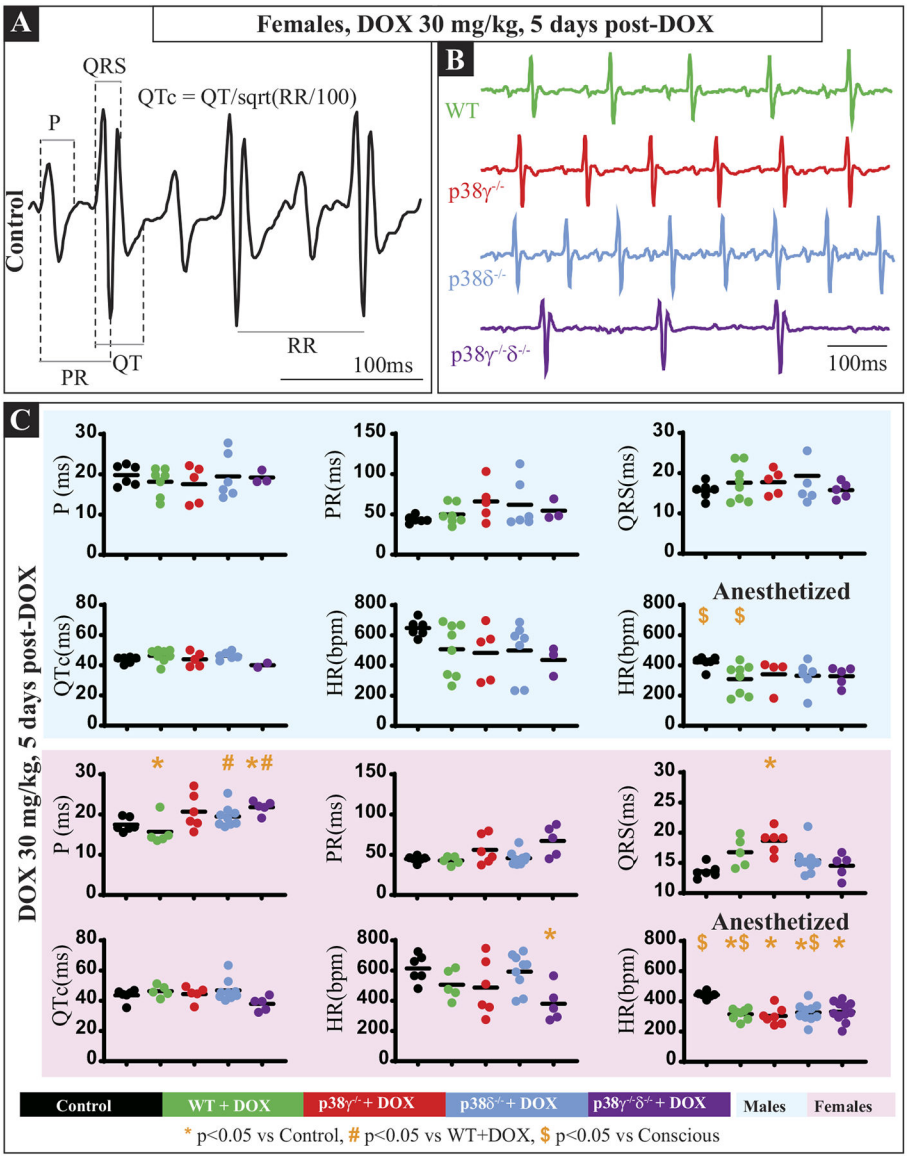

Fig. 3.

Electrocardiogram (ECG) parameters are preserved in doxorubicin (DOX)-treated female p38$\delta^{-/-}$ mice. *A*: representative ECG from a conscious female control mouse with the description of the specific parameters measured. *B*: representative ECGs from conscious female WT, p38$\gamma^{-/-}$, p38$\delta^{-/-}$, and p38$\gamma^{-/-}\delta^{-/-}$ mice treated with DOX. *C*: ECG parameters such as the P wave interval (P), P-R interval (PR), QRS duration (QRS), Q-T interval corrected for heart rate (QTc), and heart rate (HR) were measured in conscious male (*top*, blue) and female (*bottom*, pink) mice treated with 30 mg/kg DOX 5 days posttreatment. HR in anesthetized mice was also measured for comparison. Each color-coded circle corresponds to individual data point, one from each mouse. Average values are indicated by a horizontal black line. One-way ANOVA was used to determine statistically significant differences between groups for each parameter, and 2-tailed, unpaired Student's *t* tests were performed as post hoc analysis. Bonferroni correction was applied for multiple comparisons.

Health Research Alliance Author Manuscript

Due to variability in survival rates 5 days post-DOX and weaker signals from more sick mice, variable sample sizes are observed between groups and parameters, respectively. Sample sizes for each group of conscious mice are as follows: males, control: $n = 6$, WT+DOX: $n = 8$, p38$\gamma^{-/-}$+DOX: $n = 5$, p38$\delta^{-/-}$+DOX: $n = 6$, p38$\gamma^{-/-}\delta^{-/-}$+DOX: $n = 5$; females, control: $n = 6$, WT+DOX: $n = 5$, p38$\gamma^{-/-}$+DOX: $n = 6$, p38$\delta^{-/-}$+DOX: $n = 9$, p38$\gamma^{-/-}\delta^{-/-}$+DOX: $n = 5$. Samples sizes of anesthetized HR in males and females correspond to those specified in Fig. 2, echocardiographic analysis. *$P < 0.05$ vs. control. #$P < 0.05$ vs. WT+DOX. \$$P < 0.05$ vs. conscious.

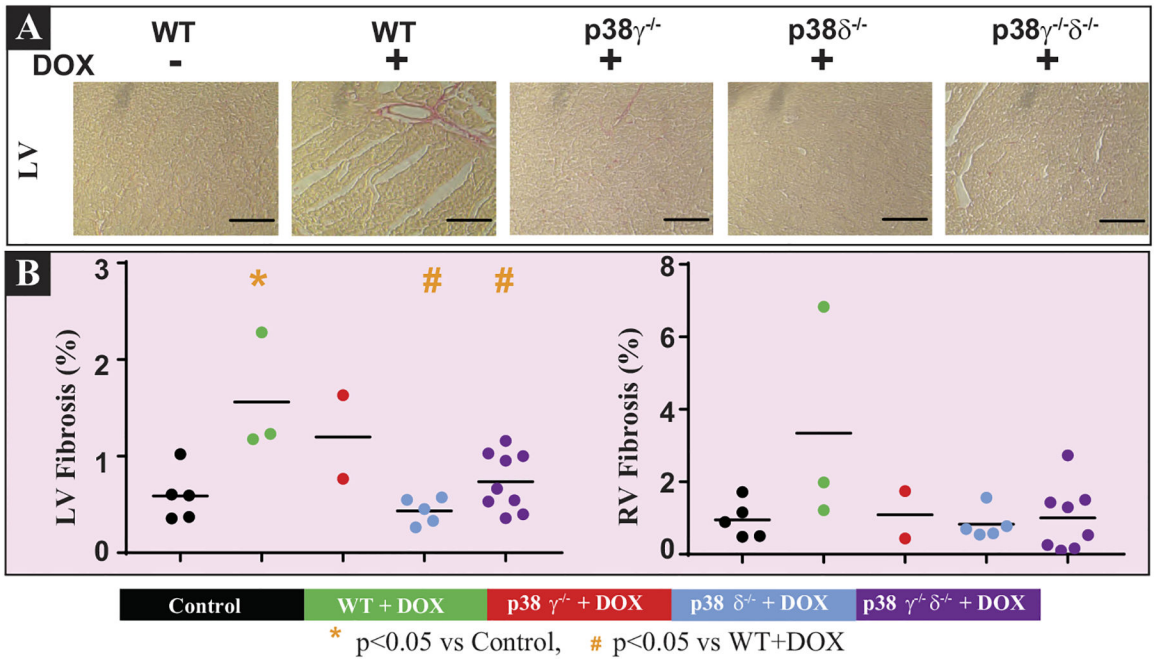

Fig. 4.

Fibrosis is reduced in left ventricles (LV) of the surviving doxorubicin (DOX)-treated female p38δ $^{-/-}$ mice. *A*: representative images of Picro Sirius Red staining in LV of female mice of the indicated genotypes treated with 30 mg/kg DOX (+) or with saline (−). Tissue samples were collected on *day 10* posttreatment. Scale bar, 100 μm. *B*: quantification of the areas occupied by fibrosis as visualized by red positive staining (collagen) in LV and right ventricles of female mice was carried out as detailed in METHODS. Each color-coded circle is the average of LV fibrosis in the base, mid and apical regions of the LV. Average values are indicated by horizontal black line. One-way ANOVA was used to determine statistically significant differences between groups for each parameter, and 2-tailed, unpaired Student's *t* tests were performed as post hoc analysis. Bonferroni correction was applied for multiple comparisons. Due to variability in survival rates 10 days post-DOX, sample sizes varied between groups. Sample sizes for each group are as follows: females, control: $n = 5$, WT+DOX: $n = 3$, p38γ$^{-/-}$+DOX: $n = 2$, p38δ$^{-/-}$+DOX: $n = 5$, p38γ$^{-/-}$δ$^{-/-}$+DOX: $n = 9$. Note: due to low sample size, caused by high mortality, the p38γ$^{-/-}$+DOX group was excluded from statistical comparisons. *$P < 0.05$ vs. control. #$P < 0.05$ vs. WT+DOX.

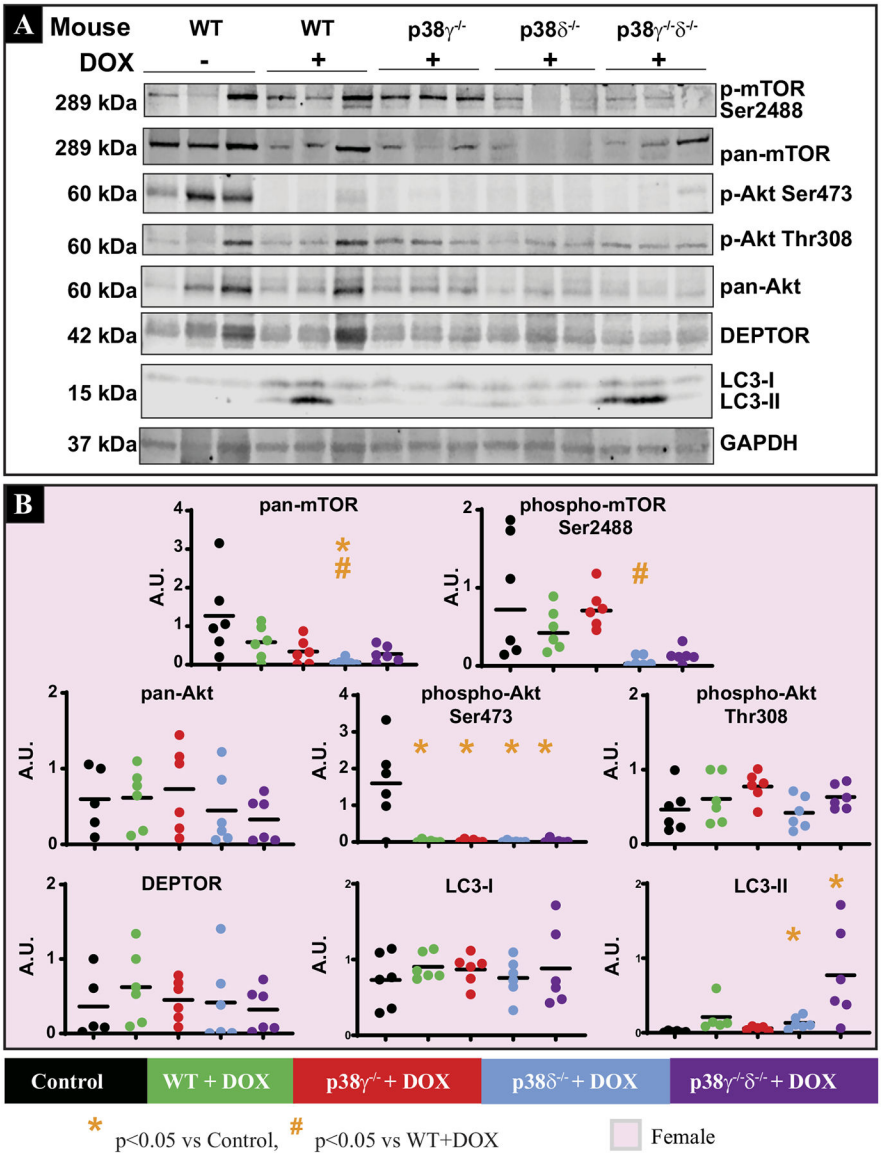

Fig. 5.

Reduced mammalian target of rapamycin (mTOR) activation and increased expression of autophagy marker LC3-II in hearts of 30 g/mg doxorubicin (DOX)-treated female p38δ$^{-/-}$ mice. Immunoblot (*A*) and relative quantification (*B*) of the specified proteins in hearts from female mice of the indicated genotypes. Tissue samples were collected on *day 10* posttreatment. Lysates from the hearts of 3 individual mice were included from each group. The quantification data include the results of 2 technical repeats of the immunoblot experiment. Each protein expression was normalized to GAPDH expression in the same sample to avoid loading errors. Each color-coded circle corresponds to individual data points. Average values are indicated by a horizontal black line. One-way ANOVA was used to determine statistically significant differences between groups for each parameter, and 2-tailed, unpaired Student's *t* tests were performed as post hoc analysis. Bonferroni

correction was applied for multiple comparisons. Each group had a sample size of $n = 3$, and 2 technical replicates/group were carried out. $*P < 0.05$ vs. control. $\#P < 0.05$ vs. WT+DOX.

Health Research Alliance Author Manuscript

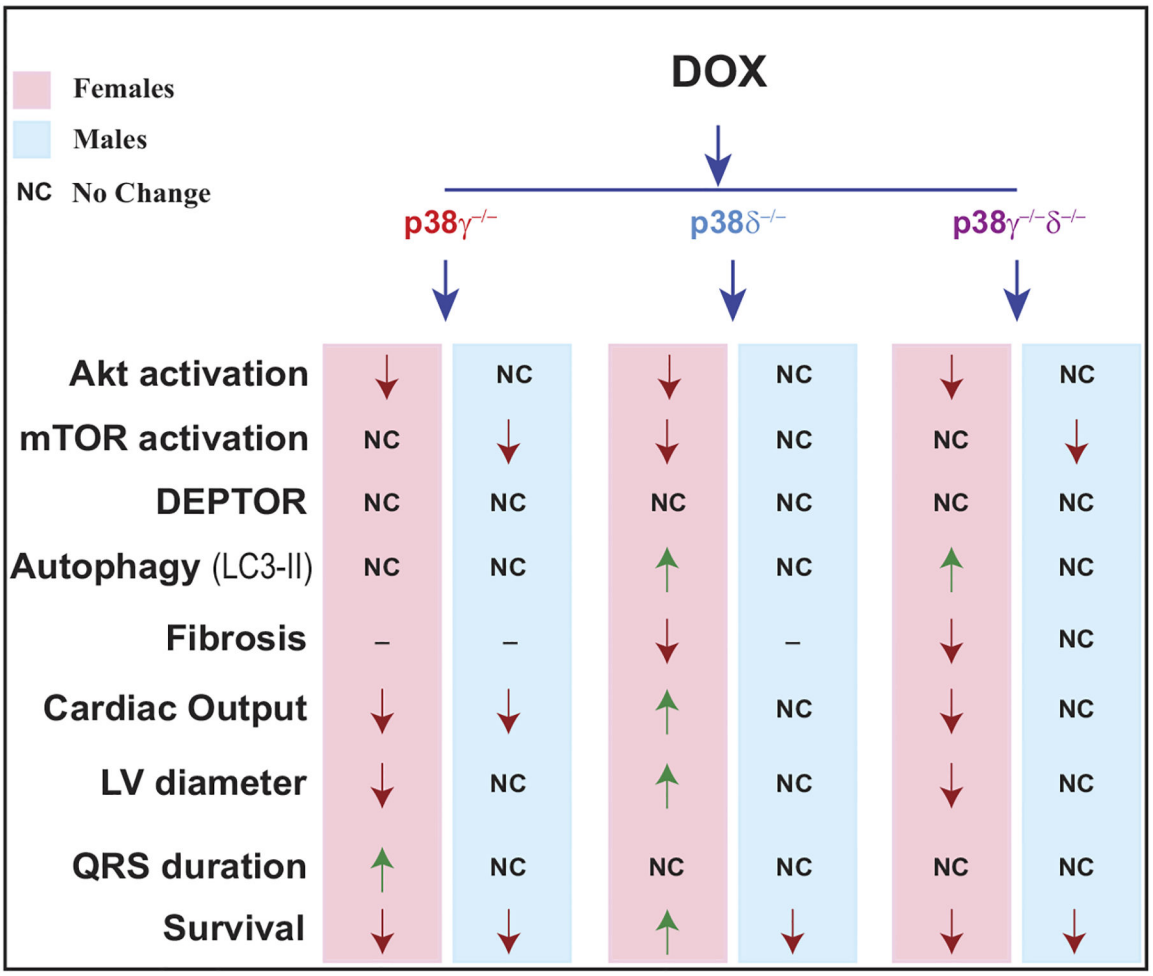

Fig. 6.

p38δ deletion increases autophagy marker expression and preserves cardiac function and survival in female mice: summary of findings.

Health Research Alliance Author Manuscript

Am J Physiol Heart Circ Physiol. Author manuscript; available in PMC 2024 April 15.

Table 1.

Summary of cardiac functional data

	Control	WT	p38$\gamma^{-/-}$	p38$\delta^{-/-}$	p38$\gamma^{-/-}\delta^{-/-}$
Males					
Echocardiography					
EF, %	62.76 ± 11.14	68.17 ± 13.48	73.24 ± 17.70	64.94 ± 17.79	73.80 ± 15.00
CO, mL/min	18.66 ± 4.35	10.86 ± 7.63	9.97 ± 5.71	9.74 ± 5.55 *	6.81 ± 4.74 *,#
FS, %	34.06 ± 8.13	38.05 ± 10.19	45.39 ± 21.47	36.65 ± 15.11	46.85 ± 24.81
LVPWD, mm	0.72 ± 0.23	0.74 ± 0.13	0.79 ± 0.07	0.88 ± 0.24	1.13 ± 0.28 #
LVPWS, mm	1.18 ± 0.37	1.12 ± 0.21	1.20 ± 0.24	1.10 ± 0.27	1.44 ± 0.19
LVEDD, mm	4.02 ± 0.38	3.32 ± 0.80	3.06 ± 0.85	3.29 ± 0.96	2.59 ± 0.96 *
LVESD, mm	2.67 ± 0.52	2.09 ± 0.70	1.80 ± 0.97	2.20 ± 1.00	1.43 ± 0.89
Electrocardiography					
P, ms	19.80 ± 2.57	18.16 ± 3.46	17.56 ± 4.69	19.49 ± 5.63	19.20 ± 1.61
PR, ms	43.78 ± 4.37	49.92 ± 12.43	66.05 ± 24.22	61.96 ± 30.51	54.58 ± 12.77
QRS, ms	15.70 ± 2.02	17.64 ± 4.53	17.77 ± 3.07	19.33 ± 7.19	15.78 ± 2.03
QTc, ms	43.64 ± 2.10	46.33 ± 4.30	43.97 ± 4.77	46.30 ± 2.47	40.06 ± 2.04
$HR_{conscious}$, beats/min	648 ± 56	507 ± 173	483 ± 180	499 ± 187	436 ± 95
$HR_{anesthetized}$, beats/min	420 ± 41$	309 ± 100$	341 ± 106	330 ± 99	328 ± 63
Females					
Echocardiography					
EF, %	54.83 ± 3.31	72.96 ± 27.37	75.04 ± 17.25	58.92 ± 11.13	71.25 ± 15.64
CO, mL/min	16.28 ± 2.57	4.43 ± 1.66 *	5.05 ± 5.14 *	9.13 ± 3.56 *,#	8.30 ± 4.44 *
FS, %	28.03 ± 2.14	47.22 ± 24.80	44.31 ± 14.97	31.06 ± 8.60	41.16 ± 12.96
LVPWD, mm	0.70 ± 0.04	0.85 ± 0.25	1.02 ± 0.18 *	0.65 ± 0.18	0.81 ± 0.24
LVPWS, mm	0.96 ± 0.10	1.18 ± 0.43	1.31 ± 0.22	0.94 ± 0.20	1.15 ± 0.32
LVEDD, mm	3.91 ± 0.15	2.46 ± 0.59 *	2.32 ± 1.06 *	3.37 ± 0.49 #	2.95 ± 0.66 *
LVESD, mm	2.81 ± 0.13	1.41 ± 0.91 *	1.40 ± 0.99 *	2.35 ± 0.52 #	1.80 ± 0.69 *
Electrocardiography					
P, ms	17.50 ± 1.71	15.71 ± 3.46 *	20.71 ± 4.36	19.51 ± 2.58 #	21.82 ± 1.61 *#

	Control	WT	p38γ$^{-/-}$	p38δ$^{-/-}$	p38γ$^{-/-}$δ$^{-/-}$
PR, ms	44.87 ± 3.89	42.79 ± 5.18	56.07 ± 17.75	45.81 ± 8.42	67.21 ± 18.82
QRS, ms	13.61 ± 1.10	16.77 ± 2.45	18.67 ± 1.96*	15.43 ± 2.35	14.54 ± 1.97
QTc, ms	43.62 ± 4.15	46.38 ± 3.83	44.47 ± 5.10	46.90 ± 7.16	37.97 ± 4.62
$HR_{conscious}$, beats/min	614 ± 91	506 ± 98	487 ± 185	593 ± 121	380 ± 118*
$HR_{anesthetized}$, beats/min	443 ± 21$^{\$}$	315 ± 36$^{*,\$}$	303 ± 56*	326 ± 61$^{*,\$}$	330 ± 63*

Values are means ± SD. WT, wild-type; DOX, doxorubicin. See the text for additional definitions.

* $P < 0.05$ vs. control,

$^{\#}$ $P < 0.05$ vs. WT + DOX30, and $\$$ $P < 0.05$ in anesthetized vs. conscious mice.